Comparison of baseline-nitrate technetium-99m-sestamibi with rest-redistribution thallium-201 tomography in detecting viable

JACC Vol. 30, No. 2
August 1997:384–91

Comparison of Baseline–Nitrate Technetium-99m Sestamibi With Rest–Redistribution Thallium-201 Tomography in Detecting Viable Hibernating Myocardium and Predicting Postrevascularization Recovery

ROBERTO SCIAGRÀ, MD, GIANNI BISI, MD, GIOVANNI M. SANTORO, MD,*
FRANCESCA ZERAUSCHEK, MD, STELVIO SESTINI, MD, PAOLA PEDENOVI, MD,*
RUGGIERO PAPPAGALLO, NMT, PIER FILIPPO FAZZINI, MD*

Florence, Italy

Objectives. **This study aimed to define the optimal criteria for detecting viable myocardium with rest–redistribution thallium-201 (Tl-201) or baseline–nitrate technetium-99m (Tc-99m) sestamibi single-photon emission computed tomography (SPECT) using discriminant analysis and to compare the accuracy of the two tracers in predicting postrevascularization recovery.**

Background. **Rest–redistribution Tl-201 imaging is currently used for detection of myocardial viability, but the optimal variables for territory classification have not yet been defined. Although Tc-99m sestamibi is reportedly less effective than Tl-201, its reliability can be increased by injecting it during nitrate infusion.**

Methods. **In 35 patients with left ventricular (LV) dysfunction, tracer activity within asynergic coronary territories was quantified on rest and redistribution Tl-201 and baseline and nitrate Tc-99m sestamibi SPECT. Asynergic territory viability was evaluated on the basis of the postrevascularization functional outcome.**

Results. **Percent activity within asynergic territories was significantly influenced by their viability ($p < 0.005$) and the type of acquisition ($p < 0.0001$) but not by the tracer used. Discriminant analysis identified redistribution Tl-201 activity and nitrate-induced Tc-99m sestamibi activity change as the two most significant predictors of postrevascularization recovery. The discriminant function defined for Tl-201, including redistribution activity and reversibility, correctly classified 38 of 56 asynergic territories, whereas that for Tc-99m sestamibi, including nitrate-induced activity change and activity in nitrate images, correctly classified 43 territories.**

Conclusions. **Redistribution activity is more important than reversibility when differentiating viable from nonviable territories using rest–redistribution Tl-201. In Tc-99m sestamibi SPECT, nitrate-induced activity changes are particularly useful in identifying myocardial viability. Baseline–nitrate Tc-99m sestamibi SPECT appears no less effective than rest–redistribution Tl-201 in predicting postrevascularization recovery.**

(J Am Coll Cardiol 1997;30:384–91)

In patients with chronic coronary artery disease (CAD) and left ventricular (LV) dysfunction, the aim of evaluating viable hibernating myocardium in asynergic regions is to predict functional recovery after coronary revascularization (1). Positron emission tomography (PET) is considered a highly accurate method for identifying viable myocardium (2–4), but recent data have questioned the value of the perfusion/metabolism mismatch and suggest that more complex absolute blood flow measurements are needed (5). Furthermore, the limited number of PET facilities and the growing demand warrant the use of less expensive and more widely available imaging modalities.

Thallium-201 (Tl-201) is considered reliable for the recognition of viable myocardium if appropriate imaging protocols are used (6–13). Among these, rest–redistribution Tl-201 scintigraphy should be particularly well suited when viability is the main diagnostic issue (6,9–13). However, the results are not homogeneous, probably owing to different imaging techniques and viability criteria. More specifically, dissimilar cutoff points of Tl-201 activity were used to distinguish viable from nonviable regions, and defect reversibility was differently considered. A thorough evaluation of the most effective rest–redistribution Tl-201 variables for the recognition of viable hibernating myocardium is still lacking.

The reliability of technetium-99m (Tc-99m) sestamibi in evaluating myocardial viability has not yet been established. The relation of Tc-99m sestamibi uptake and retention with

From the Nuclear Medicine Unit, Department of Clinical Physiopathology, University of Florence and *Division of Cardiology, Careggi Hospital, Florence, Italy. This study was presented in part at the 43rd Annual Meeting of the Society of Nuclear Medicine, Denver, Colorado, June 1996.

Manuscript received September 4, 1996; revised manuscript received April 16, 1997, accepted April 25, 1997.

Address for correspondence: Dr. Roberto Sciagrà, Nuclear Medicine Unit, Department of Clinical Physiopathology, University of Florence, Viale Morgagni 85, 50134 Florence, Italy. E-mail: r.sciagra@mednuc2.dfc.unifi.it.

0735-1097/97/$17.00
PII S0735-1097(97)00192-7

Abbreviations and Acronyms

CABG = coronary artery bypass graft surgery
CAD = coronary artery disease
EF = ejection fraction
LV = left ventricular
PET = positron emission tomography (tomographic)
PTCA = percutaneous transluminal coronary angioplasty
SPECT = single-photon emission computed tomography (tomographic)
Tc-99m = technetium-99m
Tl-201 = thallium-201
WMSI = wall motion score index

myocardial cell membrane integrity and tissue viability has been demonstrated (14–16), but human studies (11,17–21) have suggested that rest Tc-99m sestamibi could underestimate myocardial viability. Some of these reports are of limited value because they were just comparisons of defect reversibility in Tc-99m sestamibi and Tl-201 imaging (18,19). More recent data (12,22) have shown that quantitative analysis of Tc-99m sestamibi single-photon emission computed tomography (SPECT) reduces the underestimation of viability compared with Tl-201 imaging. For PET comparative studies, fluorine-18 fluorodeoxyglucose uptake within Tc-99m sestamibi defects was found to be minimal when Tc-99m sestamibi uptake was severely reduced (22,23). Few studies have compared rest Tc-99m sestamibi uptake with postrevascularization functional outcome, and their results are not homogeneous (11,12,17). In general, only minor differences between Tc-99m sestamibi and Tl-201 scintigraphy were registered (11,12).

More recently, it was suggested that modifications of the standard protocol for rest Tc-99m sestamibi might be useful (22,24,25). In particular, a relation between the increase in uptake obtained by injecting Tc-99m sestamibi during nitrate infusion and the presence of functional recovery was demonstrated (26–28). However, a comparison within the same patient cohort between baseline–nitrate Tc-99m sestamibi and rest–redistribution Tl-201 is not available. Such a comparison requires defining the optimal criteria for identification of hibernating myocardium for each imaging technique. To achieve this result, an objective approach based on discriminant analysis appears advantageous (29) because this method is not influenced by the distribution of the experimental observations in the intermediate range, where the cutoff point to differentiate viable from nonviable regions is usually defined. Discriminant analysis also allows a multivariate approach and hence can be useful in estimating which variables are important in the identification of hibernating myocardium. Accordingly, in the present study all quantitative variables derived from rest–redistribution Tl-201 and baseline–nitrate Tc-99m sestamibi SPECT were incorporated in a multivariate discriminant model to enable identification of the most useful classification criteria for the prediction of postrevascularization recovery, thereby allowing a reliable comparison of the two tracers.

Methods

Study patients. The study group was selected from patients with a previous myocardial infarction, impaired LV function (LV ejection fraction [EF] <50%) and severe regional dysfunction who were referred for perfusion SPECT in our laboratory. To be included in the study, the patients had to be scheduled for a revascularization procedure on the basis of clinical criteria and the independent judgment of the referring physician. Exclusion criteria were recent (<3 months) myocardial infarction or unstable angina; presence of heart disease other than CAD; previous revascularization procedures; and unwillingness to participate in the study. Forty-two patients were enrolled, of whom three refused the proposed intervention, another three had incomplete preoperative data, and one experienced a perioperative infarction. Thus, the study cohort included 35 patients (33 men; mean [±SD] age 58 ± 9.3 years, range 35 to 71). The results of a data-based quantitative analysis of Tc-99m sestamibi images in 18 patients were included in previous reports from our group (26,27).

According to the most recent coronary angiograms, interpreted by two experienced observers (G.M.S.) with no knowledge of the other patient data, all patients had significant (≥50% lumen narrowing) CAD. Specifically, 10 patients had one-vessel, 13 two-vessel and 12 three-vessel CAD.

Study protocol. Within 1 week, all patients underwent 1) two-dimensional echocardiography for assessment of regional wall motion and global LVEF; 2) baseline rest and nitrate Tc-99m sestamibi SPECT; and 3) rest–redistribution Tl-201 SPECT. The study sequence was randomized, with a 48-h interval between Tc-99m sestamibi and Tl-201 imaging. All patients continued receiving their current medications, with the exception of nitrates, which were discontinued 48 h before the scintigraphic examinations. No changes in the clinical conditions of any patient were registered during the time needed to conclude the study protocol.

Complete revascularization of all stenotic major epicardial branches of the coronary arteries was achieved by either coronary artery bypass graft surgery (CABG) (16 patients) or percutaneous transluminal coronary angioplasty (PTCA) (19 patients). After revascularization (3 months for CABG, 1 month for PTCA), two-dimensional echocardiography was repeated to assess regional wall motion and LVEF changes. In the case of PTCA, restenosis was also previously excluded by negative exercise stress test results.

The study protocol was approved by the ethics committee for human studies at our institution. All patients gave informed consent to participate in the study.

Two-dimensional echocardiography. An Aloka SSD-870 echocardiograph with 2.5- to 3.5-MHz transducers was used to acquire both the pre- and the postrevascularization studies, which were analyzed by two experienced observers (G.M.S., P.P.) who had no knowledge of the other data or the acquisition sequence. For wall motion analysis, the LV was divided into 13 segments (26,30), and wall motion and thickening of each segment were scored as follows: 1 = normal; 2 =

hypokinesia; 3 = akinesia; 4 = dyskinesia (30,31). Discrepancies were resolved by consensus. The asynergic segments were assigned to the appropriate coronary artery territory, and for each territory a wall motion score index (WMSI) was derived from the following formula: Total score of asynergic segments/Number of asynergic segments.

The evolution of regional wall motion in the asynergic coronary territories was assessed by comparing the WMSI before and after revascularization. A significant improvement was defined by a postrevascularization improvement in two or more continuous segments of the asynergic territory and a WMSI decrease >0.22 compared with the prerevascularization value (26,31).

Tl-201 SPECT. Patients were studied after an overnight fast, with the injection at rest of 3 mCi (111 MBq) of Tl-201 followed 15 to 30 min later by SPECT acquisition. The redistribution images were collected after a 3- to 4-h delay. Both studies were acquired using an Elscint Apex SP4 gamma camera equipped with a low-energy all-purpose collimator, with a 15% window centered on the 68- to 80-keV peak and a second 10% window centered on the 167-keV peak of Tl-201. Sixty projections of 25 s each were collected in step and shoot mode over a 180° arc (from the 45° right anterior oblique to the 45° left posterior oblique projection) on a 64 × 64 matrix. Filtered backprojection using a Butterworth filter with a 0.35 cutoff and an order of 5.0 was used to reconstruct the transaxial slices, which were then realigned along the heart axis.

Tc-99m sestamibi SPECT. Baseline rest and nitrate studies were performed in random sequence on two different days with a 24-h interval. The tracer dose was 20 to 25 mCi (740 to 925 MBq) in both instances. For the nitrate study, 10 mg of isosorbide dinitrate diluted in 100 ml of isotonic saline solution was infused over 20 min to the patient lying supine during electrocardiographic and blood pressure monitoring (26,27). As soon as systolic blood pressure dropped >20 mm Hg (eight patients), or a systolic blood pressure value <90 mm Hg was measured (six patients), Tc-99m sestamibi was injected. If none of these two criteria was fulfilled, the tracer was injected 15 min after the start of infusion, and the infusion was maintained for a further 2 min (21 patients).

Images were collected 60 min later using the same gamma camera as for Tl-201, equipped with an ultrahigh resolution collimator, and with a 20% window centered on the 140-keV photopeak of Tc-99m. Sixty projections of 20 s each were acquired. Image reconstruction was performed using backprojection without a preprocessing filter and with a Wiener reconstruction filter. No attenuation or scatter correction was used. The transaxial slices were realigned along the heart axis.

Quantitative analysis. For quantitative evaluation of SPECT images, the short-axis slices from the first with apical activity to the last with activity at the base were used. Their count profiles were generated by computer software and plotted onto a two-dimensional volume-weighted polar map that was then divided into 13 segments that matched the echocardiographic segments. Using an automated procedure, segment tracer activity was calculated as the total of the normalized counts of the pixels divided by the number of pixel included within the segment. The segment with maximal activity was then normalized to 100, and the activity of the other segments was expressed as a percent of the peak activity segment. To define the mean activity of the coronary artery territories with abnormal pre-revascularization WMSI, only the segments corresponding to the asynergic ones were identified, and a mean asynergic territory percent activity was derived according to the following formula: Total percent activity of asynergic segments/Number of asynergic segments.

Finally, the difference between redistribution and rest Tl-201 mean percent activity (reversibility) and, respectively, nitrate and baseline Tc-99m sestamibi mean percent activity (nitrate-induced change) was calculated and expressed as a percentage of the rest or the baseline value.

Statistical analysis. Results are expressed as mean value ± SD. Analysis of variance with the Tukey post hoc test was used for between- and within-group comparisons. Comparison of proportions was made using the Fisher exact test. Stepwise linear discriminant analysis was performed on the various data sets obtained using the two tracers to determine which variables or combination thereof best discriminated between viable and nonviable regions. This procedure involves the calculation of a linear function that yields the most optimal possible classification of the observations having as its reference a grouping factor, which in the present case was the presence of postrevascularization functional recovery. The achieved classification was then submitted to a jackknife validation procedure to limit bias in the number of patients correctly classified (32). The most effective discriminant function was finally selected by taking into account the highest canonical correlation and the most accurate cross-validated classification of the asynergic regions. The classification after cross-validation was also used to calculate the predictive values of the two imaging modalities. The STATISTICA and Minitab statistical software packages were used for data analysis. A p value <0.05 was considered statistically significant.

Results

General findings. Of 455 echocardiographic segments in 35 patients, 273 had abnormal wall motion and were included in 56 coronary artery territories, all related to stenotic vessels. The pre-revascularization WMSI of these 56 coronary territories was 2.5 ± 0.5. Severe wall motion abnormality with a prevalence of akinetic or dyskinetic segments (WMSI ≥2.5) was observed in 36 of 56 territories. The pre-revascularization global LVEF was 36.1 ± 8.4% (range 18% to 49%). In 30 territories the postrevascularization echocardiogram fulfilled the criteria for a significant functional recovery (WMSI decreased from 2.5 ± 0.4 to 1.7 ± 0.5); these territories were therefore considered to include viable hibernating myocardium. The WMSI of the 26 remaining asynergic coronary territories remained unchanged (2.5 ± 0.5 both before and after revascularization), and they were defined as nonviable. A pre-revascularization WMSI ≥2.5 was observed in 21 viable

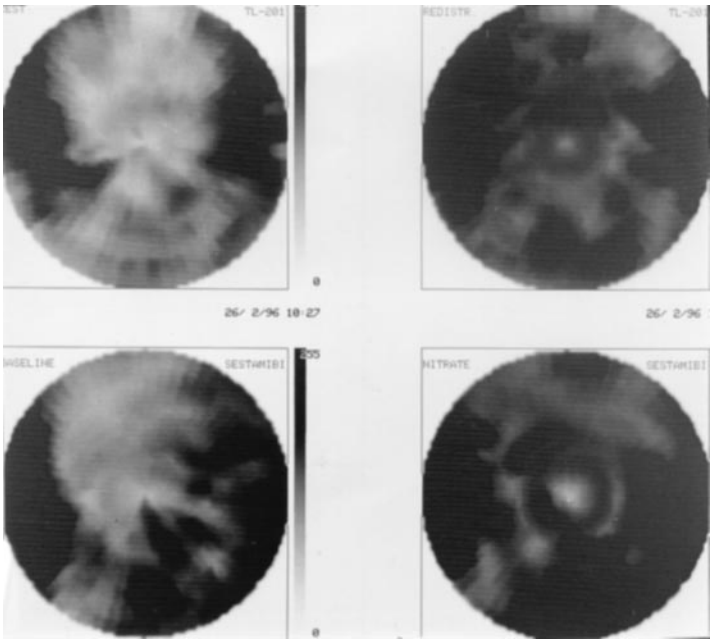

Figure 1. Polar map displays of patient with two-vessel CAD, anterior akinesia and inferior hypokinesia. Reduced tracer uptake is present on both rest Tl-201 (**top left**) and baseline Tc-99m sestamibi (**bottom left**). A clear gain in tracer activity is observed on both redistribution Tl-201 (**top right**) and nitrate Tc-99m sestamibi (**bottom right**). After two-vessel coronary angioplasty, significant functional recovery was registered in both the anterior and inferior walls.

and 15 nonviable territories. After revascularization, global LVEF increased in 23 patients (from 36.2 ± 8% to 45.8 ± 8.3%, range 3 to 22), whereas it remained unchanged or worsened (from 36 ± 9.5% to 32.3 ± 8.4%) in the remaining 12 patients.

SPECT. A typical example of rest–redistribution Tl-201 and baseline–nitrate Tc-99m sestamibi polar map displays is shown in Figure 1.

A three-way analysis of variance with repeated measures for percent activity in the asynergic territories (grouping factor: viability [presence or absence of postrevascularization recovery]; repeated measure factors: tracer [Tl-201 or Tc-99m sestamibi] and type of study [rest or redistribution and baseline or nitrate, respectively]) was performed. This analysis showed a significant viability effect ($F = 10.08$, $p < 0.005$) and an even more significant study effect ($F = 17.98$, $p < 0.0001$), but no tracer effect could be demonstrated.

In the rest study, Tl-201 activity in the 56 asynergic territories was 62.3 ± 11.2% (66.2 ± 9.5% in viable, 57.7 ± 11.4% in nonviable territories, $p < 0.0002$). In the redistribution images, Tl-201 activity was 65.5 ± 12.5% ($p < 0.0002$ vs. rest). The activity in the 30 viable territories increased to 71 ± 10% ($p < 0.0002$ vs. rest) and to 59.1 ± 12.1% ($p = 0.79$ vs. rest) in the 26 nonviable regions: A significant difference between the two groups (viable and nonviable) was registered ($p < 0.0002$) (Fig. 2). Among the nonviable territories, normal (≥75%) rest and redistribution activity was found only in two territories with WMSI <2.5. Reversibility was close to being statistically different between the two groups (viable 7.2 ± 8.9% vs. nonviable 2 ± 7.4%, $p = 0.056$). The rate of significant (>10%) reversibility was 33% (10 of 30) within the viable and 15% (4 of 26) within the nonviable group ($p = 0.21$).

In the 56 asynergic territories, rest Tc-99m sestamibi activity was 63.4 ± 14.6% ($p = 0.23$ vs. rest Tl-201; $p < 0.02$ vs. redistribution Tl-201), 66 ± 13.7% in the viable ($p = 0.99$ vs. rest Tl-201; $p < 0.0002$ vs. redistribution Tl-201) and 60.3 ± 15.2% in the nonviable territories ($p = 0.10$ vs. rest Tl-201; $p = 0.87$ vs. redistribution Tl-201). A significant difference was hence registered between the two groups ($p < 0.0002$). On nitrate images, the activity of all territories was 65.5 ± 15.1% ($p < 0.02$ vs. baseline activity). This value was not different from that of redistribution Tl-201 ($p = 1$) but was significantly higher than that of rest Tl-201 ($p < 0.0002$). A significant

Figure 2. Rest and redistribution Tl-201 percent activity in asynergic coronary territories grouped according to postrevascularization recovery. Individual data points are represented by **plus signs** if the prerevascularization WMSI was <2.5 and by **diamonds** if ≥2.5. Mean value ± SD is also shown.

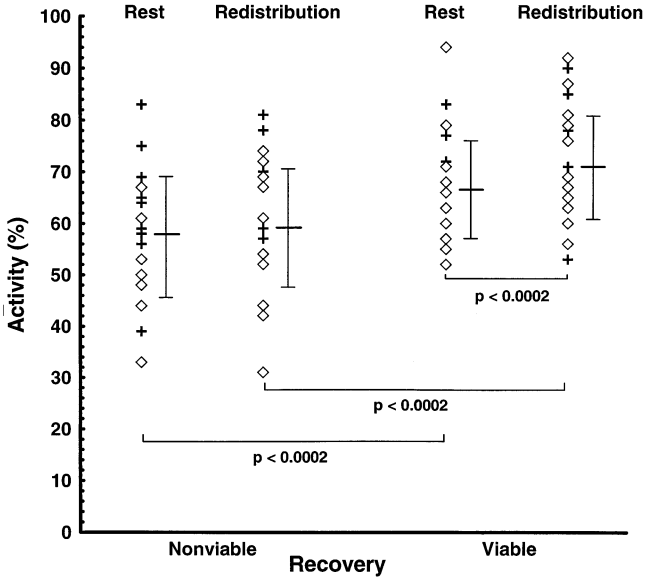

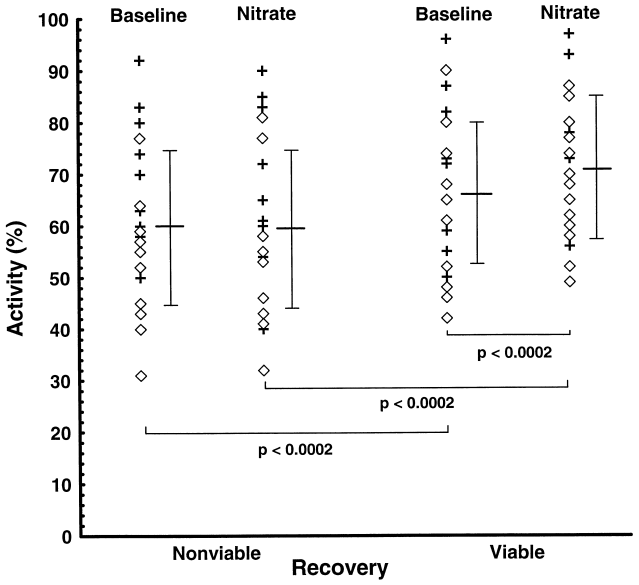

Figure 3. Baseline and nitrate Tc-99m sestamibi percent activity in asynergic coronary territories grouped according to postrevascularization recovery. Format and symbols as in Figure 2.

difference between viable and nonviable territories was also observed in nitrate activity (70.6 ± 13.2% vs. 59.5 ± 15.3%, $p < 0.0002$) (Fig. 3). Nitrate activity in the viable territories was significantly higher than that of baseline Tc-99m sestamibi ($p < 0.0002$) and rest Tl-201 ($p < 0.0005$) in the same territories. No significant difference was found in comparison with redistribution Tl-201 activity ($p = 0.99$). Among the nonviable territories, normal rest activity was found in six cases (three with WMSI <2.5, three with WMSI ≥2.5) and normal nitrate activity in six (four with WMSI <2.5, two with WMSI ≥2.5). The nitrate-induced change was substantially higher in the viable than in the nonviable group (7.9 ± 10.1% vs. −1.1 ± 8.7%, $p < 0.0005$). A >10% nitrate-induced activity increase was registered in 10 (33%) of 30 viable territories and in none of 26 nonviable territories ($p < 0.001$). Only 3 of 10 territories with >10% activity increase had >10% reversibility on Tl-201 SPECT.

Discriminant analysis. Table 1 shows the results of discriminant analysis for Tl-201 rest–redistribution imaging. Among the three variables examined, redistribution Tl-201 was the most significant in univariate analysis, with a cutoff value for viability >65% of peak activity. When all three Tl-201 variables were submitted to stepwise discriminant analysis, a classification function based on a two-variable model that included redistribution activity and reversibility was defined, and the derived classification matrix after cross-validation correctly classified 21 hibernating and 17 nonviable territories (Fig. 4). Thus, the overall accuracy of rest–redistribution Tl-201 SPECT, according to discriminant analysis, was 68%, with a 70% positive and a 65% negative predictive value. With regard to the territories with WMSI ≥2.5, 10 (67%) of 15 were correctly classified as nonviable and 15 (71%) of 21 as viable. In practice, by also taking reversibility into account, it was possible to correctly reclassify four territories that were wrongly categorized using the redistribution activity threshold.

Table 2 shows the results of discriminant analysis for Tc-99m sestamibi baseline–nitrate imaging. On univariate analysis, nitrate-induced change and nitrate activity were the two significant predictors of postrevascularization recovery. The related cutoff values were +3.5% or greater change and more than 65% of peak activity, respectively. Stepwise discriminant analysis selected both nitrate-induced change and nitrate activity as significant predictors of postrevascularization recovery. According to the derived function and after cross-validation, 23 viable and 20 nonviable territories were correctly classified (Fig. 5). Therefore, the overall accuracy of Tc-99m sestamibi baseline–nitrate imaging according to discriminant

Table 1. Results of Discriminant Analysis for Rest–Redistribution Thallium-201 Single-Photon Emission Computed Tomography

	Univariate Analysis			
			Classification Matrix	
	F Value	p Value	TP	TN
Rest	9.17	< 0.005	22 (20*)	16
Red	16.14	< 0.0002	18	16
Rev	5.61	< 0.05	17	20

	Stepwise Multivariate Analysis						
						Classification Matrix	
	Step	F Value	p Value	Can Corr	p Value	TP	TN
Red	1	16.14	< 0.0002				
Rev	2	1.29	0.25				
Function				0.498	< 0.001	22 (21*)	17

*After jackknife cross-validation. Can Corr = canonical correlation of the discriminant function; Rest = rest thallium-201 activity; Red = redistribution thallium-201 activity; Rev = reversibility; TN = true negative (nonviable); TP = true positive (viable).

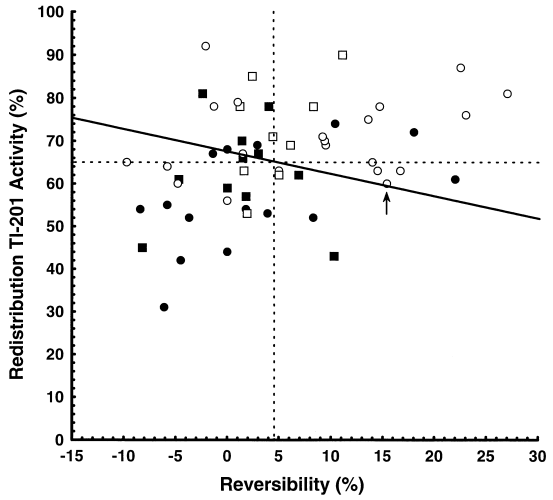

Figure 4. Scatterplot showing the relation between reversibility and redistribution Tl-201 activity. The individual data points are represented by **squares** for pre-revascularization WMSI <2.5 and by **circles** for WMSI ≥2.5. **Solid circles and squares** represent nonviable and **open circles and squares** viable territories. **Continuous line** indicates the discriminant function; **dashed lines** indicate the cutoff thresholds of the two variables as determined by univariate analysis; **arrow** points to a territory that was reclassified after jackknife cross-validation.

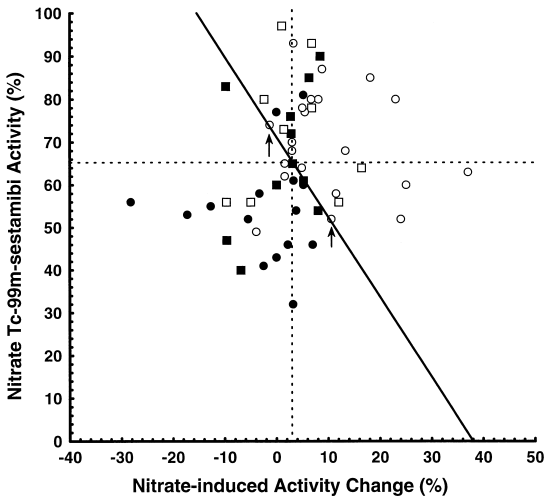

Figure 5. Scatterplot showing the relation between nitrate-induced change and nitrate Tc-99m sestamibi activity. Format and symbols as in Figure 4.

analysis was 77% (p = 0.05 vs. baseline Tc-99m sestamibi and vs. redistribution Tl-201, p = 0.07 vs. nitrate Tc-99m sestamibi and nitrate-induced Tc-99m sestamibi activity change), with a 79% positive and a 74% negative predictive value. With regard to the territories with WMSI ≥2.5, 13 (87%) of 15 were correctly classified as nonviable and 16 (76%) of 21 as viable. In practice, the territories with an activity increase greater than +10% could be regarded as viable and those with an activity decrease as nonviable; for those with activity change greater than 0 but less than +10%, the activity cutoff on nitrate images could be used for classification.

Discussion

Observations of present study. To compare rest–redistribution Tl-201 and baseline–nitrate Tc-99m sestamibi SPECT within the same patient cohort, we evaluated the quantitative variables that can be derived from the two imaging modalities to detect the factors that best explain their variability and then performed multivariate discriminant analysis to assess their relative role in predicting postrevascularization recovery.

Our data show that percent activity within an asynergic territory was significantly influenced by viability and type of acquisition (rest or redistribution for Tl-201 and baseline or nitrate for Tc-99m sestamibi). In contrast, the tracer used did not affect activity values. This finding suggests not only that no major differences exist between Tl-201 and Tc-99m sestamibi in viability detection, but also that for the latter agent it is

Table 2. Results of Discriminant Analysis for Baseline–Nitrate Technetium-99m Sestamibi Single-Photon Emission Computed Tomography

	Univariate Analysis			
			Classification Matrix	
	F Value	p Value	TP	TN
B	2.14	0.14	17	17
Nitr	8.47	< 0.01	17	19 (18*)
Change	12.64	< 0.001	18	18 (17*)

	Stepwise Multivariate Analysis						
						Classification Matrix	
	Step	F Value	p Value	Can Corr	p Value	TP	TN
Change	1	12.64	< 0.001				
Nitr	2	5.78	< 0.02				
Function				0.52	< 0.0005	25 (23*)	20

*After jackknife cross-validation. B = baseline technetium-99m sestamibi activity; Change = nitrate-induced activity change; Nitr = nitrate technetium-99m sestamibi activity; other abbreviations as in Table 1.

useful to modify the standard acquisition protocol when viability is the diagnostic issue.

In Tl-201 SPECT, redistribution activity was the most significant predictor of postrevascularization recovery according to univariate discriminant analysis, but the prediction of the postrevascularization outcome was suboptimal. The fair accuracy of rest–redistribution Tl-201 SPECT was confirmed by stepwise discriminant analysis, which identified a discriminant function, including both redistribution activity and reversibility.

Both nitrate-induced change and nitrate Tc-99m sestamibi activity were significant predictors of postrevascularization recovery, and the prediction of the functional outcome was not significantly different from that of rest–redistribution Tl-201. However, the most interesting result of this study was that stepwise analysis defined a discriminant function, including nitrate-induced change and nitrate Tc-99m sestamibi activity, which classified the territories with an accuracy superior to that achieved by rest–redistribution Tl-201. It is also remarkable that the territories with more severe wall motion abnormalities, for which the issue of myocardial hibernation was more meaningful, were correctly classified by baseline–nitrate Tc-99m sestamibi in 81% of cases and by rest–redistribution Tl-201 in 69% only.

Comparison with previous studies. Comparison of our results with previous studies is difficult because of the different segmentation (coronary territories instead of single segments) and data analysis (discriminant function instead of activity threshold). Furthermore, due to the small patient cohort, wide confidence intervals have to be considered for each result. Our Tl-201 and baseline Tc-99m sestamibi results are close to previous planar studies (6,9–11,17) but are probably worse than those obtained using SPECT (12,13). However, the influence of the data analysis method is easily understood by considering that both Udelson et al. (12) and Charney et al. (13) achieved the same high predictive values for rest–redistribution Tl-201 SPECT using completely different cutoff points for myocardial viability (60% and 25% of maximum, respectively). Despite the excellent results by Udelson et al. (12), the limitations of baseline Tc-99m sestamibi SPECT are also stressed by reports (22,25) that describe the possibility of enhancing tracer uptake by delayed imaging. With regard to nitrate Tc-99m sestamibi imaging, our results in severely asynergic regions compare well with those obtained by Maurea et al. (28).

Limitations of the study. The small patient cohort is a major limitation, as in most other reports including postrevascularization follow-up data. The study cohort was selected on the basis of the decision to proceed to coronary revascularization and did not include consecutive patients with regional asynergia and LV dysfunction. Thus, it does not represent a standard population, but a similar selection bias is often encountered (6,9–13,17). Regional wall motion was assessed visually and subjectively. However, this qualitative approach has been widely adopted for clinical studies with stress echocardiography in patients with CAD (33). The spatial agreement between echocardiography and SPECT is another important problem. The analysis based on entire coronary vascular territories instead of single segments should inherently limit the possibility of discrepant results. This choice is defensible from the clinical point of view as well because it permits the direct translation of SPECT data in terms of decision making about revascularization of the major coronary epicardial branches. Postrevascularization perfusion images were not part of this protocol. Thus, unsuccessful revascularization cannot be excluded and could explain some false positive results. This possibility was limited by the attentive evaluation of the clinical and follow-up data and by the negative exercise stress test results in the case of PTCA. Moreover, this limitation should not influence the comparison between Tl-201 and Tc-99m sestamibi. Finally, the lack of wall motion recovery does not necessarily imply the absence of viable myocardium. For instance, normally perfused tissue may coexist with subendocardial scarring. The resulting wall motion abnormality is not expected to improve, but viability would be detected by perfusion imaging. This occurrence cannot be excluded in our patients, particularly in hypokinetic regions, and could account for part of the false positive results.

Conclusions and clinical implications. The results of the present study do not support the notion of a significant inferiority of Tc-99m sestamibi compared with Tl-201 in the recognition of viable hibernating myocardium when appropriate operative sequences are used for each tracer. Our data indicate that rest–redistribution Tl-201 SPECT is a fairly effective method for the prediction of postrevascularization recovery. According to discriminant analysis, the most valuable variable in differentiating viable from nonviable myocardium is percent activity in the redistribution images, whereas defect reversibility is by far less important. Conversely, the most significant predictor of postrevascularization recovery using baseline–nitrate Tc-99m sestamibi imaging is the nitrate-induced activity change, with nitrate percent activity as a secondary significant predictor. Using the combination of the two variables in a discriminant function, Tc-99m sestamibi SPECT effectively differentiates viable from nonviable asynergic territories, with a predictive accuracy that does not appear lower than that obtained using rest–redistribution Tl-201 imaging.

References

1. Rahimtoola SH. The hibernating myocardium. Am Heart J 1988;117:211–21.
2. Tillisch JH, Brunken R, Marshall R, et al. Reversibility of cardiac wall motion abnormalities predicted by positron tomography. N Engl J Med 1986;314:884–8.
3. Brunken RC, Schwaiger M, Grover-McKay M, Phelps ME, Tillisch J, Schelbert HR. Positron emission tomography detects tissue metabolic activity in myocardial segments with persistent thallium perfusion defects. J Am Coll Cardiol 1987;10:557–67.
4. Tamaki N, Ohtani H, Yamashita K, et al. Metabolic activity in the areas of new fill-in after thallium-201 reinjection: comparison with positron emission tomography using fluorine-18 deoxyglucose. J Nucl Med 1991;32:673–8.
5. Grandin C, Wijns W, Melin JA, et al. Delineation of myocardial viability with PET. J Nucl Med 1995;36:1543–52.

6. Iskandrian AS, Hakki A, Kane SA, Goel IP, Mundth ED, Segal BL. Rest and redistribution thallium-201 myocardial scintigraphy to predict improvement in left ventricular function after coronary artery bypass grafting. Am J Cardiol 1983;51:1312–6.
7. Kiat H, Berman DS, Maddahi J, et al. Late reversibility of tomographic myocardial thallium-201 defects: an accurate marker of myocardial viability. J Am Coll Cardiol 1988;12:1456–63.
8. Dilsizian V, Rocco TP, Freedman NM, Leon MB, Bonow RO. Enhanced detection of ischemic but viable myocardium by the reinjection of thallium after stress-redistribution imaging. N Engl J Med 1990;323:141–6.
9. Mori T, Minamiji K, Kurogane H, Ogawa K, Yoshida Y. Rest-injected thallium-201 imaging for assessing viability of severe asynergic regions. J Nucl Med 1991;32:1718–24.
10. Ragosta M, Beller GA, Watson DD, Kaul S, Gimple LW. Quantitative planar rest-redistribution 201Tl imaging in detection of myocardial viability and prediction of improvement in left ventricular function after coronary bypass surgery in patients with severely depressed left ventricular function. Circulation 1993;87:1630–41.
11. Marzullo P, Parodi O, Reisenhofer B, et al. Value of rest thallium-201/technetium-99m sestamibi scans and dobutamine echocardiography for detecting myocardial viability. Am J Cardiol 1993;71:166–72.
12. Udelson JE, Coleman PS, Metherall J, et al. Predicting recovery of severe regional ventricular dysfunction: comparison of resting scintigraphy with 201Tl and 99mTc-sestamibi. Circulation 1994;89:2552–61.
13. Charney R, Schwinger ME, Chun J, et al. Dobutamine echocardiography and resting-redistribution thallium-201 scintigraphy predicts recovery of hibernating myocardium after coronary revascularization. Am Heart J 1994;128:864–9.
14. Piwnica-Worms D, Kronauge JF, Chiu ML. Uptake and retention of hexakis (2-methoxyisobutyl isonitrile) technetium(I) in cultured chick myocardial cells. Mitochondrial and plasma membrane potential dependence. Circulation 1990;82:1826–38.
15. Sinusas AJ, Trautman KA, Bergin JD, et al. Quantification of area at risk during coronary occlusion and degree of myocardial salvage after reperfusion with technetium-99m methoxyisobutyl isonitrile. Circulation 1990;82:1424–37.
16. Beanlands RSB, Dawood F, Wen W-H, et al. Are the kinetics of technetium-99m methoxyisobutyl isonitrile affected by cell metabolism and viability? Circulation 1990;82:1802–14.
17. Marzullo P, Sambuceti G, Parodi O. The role of sestamibi scintigraphy in the radioisotopic assessment of myocardial viability. J Nucl Med 1992;33:1925–30.
18. Cuocolo A, Pace L, Ricciardelli B, Chiariello M, Trimarco B, Salvatore M. Identification of viable myocardium in patients with chronic coronary artery disease: comparison of thallium-201 scintigraphy with reinjection and technetium-99m-methoxyisobutyl isonitrile. J Nucl Med 1992;33:505–11.
19. Dondi M, Tartagni F, Fallani F, et al. A comparison of rest sestamibi and rest-redistribution thallium single photon emission tomography: possible implications for myocardial viability detection in infarcted patients. Eur J Nucl Med 1993;20:26–31.
20. Sawada SG, Allman KC, Muzik O, et al. Positron emission tomography detects evidence of viability in rest technetium-99m-sestamibi defects. J Am Coll Cardiol 1994;23:92–8.
21. Soufer R, Dey HM, Ng CK, Zaret BL. Comparison of sestamibi single-photon emission computed tomography with positron emission tomography for estimating left ventricular myocardial viability. Am J Cardiol 1995;75:1214–9.
22. Dilsizian V, Arrighi JA, Diodati JG, et al. Myocardial viability in patients with chronic coronary artery disease: comparison of 99mTc-sestamibi with thallium reinjection and [18F] fluorodeoxyglucose. Circulation 1994;89:578–87.
23. Altehoefer C, von Dahl J, Biedermann M, et al. Significance of defect severity in technetium-99m-MIBI SPECT at rest to assess myocardial viability: comparison with fluorine-18-FDG PET. J Nucl Med 1994;35:569–74.
24. Worsley DF, Fung AY, Jue J, Burns RJ. Identification of viable myocardium with technetium-99m-MIBI infusion. J Nucl Med 1995;36:1037–9.
25. Maurea S, Cuocolo A, Soricelli A, et al. Myocardial viability index in chronic coronary artery disease: technetium-99m-methoxy isobutyl isonitrile redistribution. J Nucl Med 1995;36:1953–60.
26. Bisi G, Sciagrà R, Santoro GM, Fazzini PF. Rest technetium-99m sestamibi tomography in combination with short-term administration of nitrates: feasibility and reliability for prediction of postrevascularization outcome of asynergic territories. J Am Coll Cardiol 1994;24:1282–9.
27. Bisi G, Sciagrà R, Santoro GM, Rossi V, Fazzini PF. Technetium-99m-sestamibi imaging with nitrate infusion to detect viable hibernating myocardium and predict postrevascularization recovery. J Nucl Med 1995;36:1994–2000.
28. Maurea S, Cuocolo A, Soricelli A, et al. Enhanced detection of viable myocardium by technetium-99m-MIBI imaging after nitrate administration in chronic coronary artery disease. J Nucl Med 1995;36:1945–52.
29. Hill TC, Holman BL. Discriminant function analysis: toward a more rigorous approach to SPECT interpretation. J Nucl Med 1994;35:1455–6.
30. Picano E, Marzullo P, Gigli G, et al. Identification of viable myocardium by dipyridamole-induced improvement in regional left ventricular function assessed by echocardiography in myocardial infarction and comparison with thallium scintigraphy at rest. Am J Cardiol 1992;70:703–10.
31. Smart SC, Sawada S, Ryan T, et al. Low-dose dobutamine echocardiography detects reversible dysfunction after thrombolytic therapy of acute myocardial infarction. Circulation 1993;88:405–15.
32. Afifi AA, Clark V. Computer-Aided Multivariate Analysis. New York: Von Nostrand Company, 1984:246–286.
33. Armstrong W. Echocardiography in coronary heart disease. Prog Cardiovasc Dis 1988;30:267–88.